

# The spectrum and competition of autowaves in a wide-aperture laser with a saturable filter

A P Zaikin

**Abstract.** The lasing dynamics of a wide-aperture laser with an intracavity saturable absorber is theoretically studied. The saturable absorber inserting gives rise to an autowave profile of the optical field. The characteristic equation for the perturbations of the laser field is derived and solved. The spatial spectrum of autowaves is determined. The relevant set of equations was numerically solved for two types of resonant boundary conditions: total reflection of light from the side boundaries of the cavity and a coaxial laser geometry.

## 1. Introduction

Wide-aperture lasers are capable of generating light beams with complex time-dependent transverse profiles. When a saturable absorber is placed inside the cavity of such a laser, lasing may occur either in the pulsed or continuous-wave regime. Even an elementary point model of such a system is still to be adequately explored.

New regimes of lasing arising in systems with large transverse sizes have been recently revealed within the framework of a distributed model. It is of considerable interest to analyse the qualitative difference between these regimes of lasing.

In lasers with sufficiently wide apertures, where the Fresnel parameter may be of the order of several tens, regular structures may appear in the profile of a laser beam. Specifically, isolated islands of lasing—laser autosolitons [1]—may arise in the bistability region. When the gain is high, periodic wave structures may also appear. The properties of such autowaves in lasers with infinite apertures were examined in [2]. Some specific features of finite-aperture lasers were studied in [3]. No detailed analysis of the spectral composition of autowaves was performed in [2, 3], although such an analysis would be extremely important for forecasting the behaviour of laser systems.

In this paper, we investigate the spatiotemporal spectrum of autowaves in the radiation field of a wide-aperture laser with a saturable absorber. The active and nonlinear media were considered within the framework of a two-level model. We will study the dynamics of the laser field in the case when the field is totally reflected from the edges of the aperture, i.e.,

in the case of mirror side boundaries of the system. We will also consider a laser with a coaxial geometry (when the active medium has a ring-shaped cross section).

## 2. The spectrum of autowaves

The set of equations governing the optical field in a laser with a saturable absorber can be found, for example, in [2]. Using dimensionless variables, we can represent these equations in the following form:

$$\frac{\partial E}{\partial t} - i \frac{\partial^2 E}{\partial x^2} = \frac{\nu}{2} E(N - N_f - 1), \quad (1)$$

$$\frac{dN}{dt} = N_e - N(1 + I), \quad (2)$$

$$\tau \frac{dN_f}{dt} = N_{fe} - N_f(1 + I\delta). \quad (3)$$

Here,  $\nu$  is the ratio of the lifetimes of inversion and field decay in the cavity;  $N$  and  $N_f$  are the population differences of two-level particles in the active and nonlinear media, respectively;  $N_e$  and  $N_{fe}$  are the same population differences in the absence of lasing;  $E$  and  $I = |E|^2$  are the amplitude and the intensity of the laser field, respectively;  $\tau$  is the ratio of population relaxation times in the active and nonlinear media; and  $\delta$  is the ratio of saturation intensities of the active and nonlinear media.

The set of equations (1)–(3) describes the dynamics of lasers that belong to class B. The autowave phenomena predicted by these equations occur only within some (sufficiently broad) range of parameters [3]. The possibility of autowave generation in a real CO<sub>2</sub> laser was demonstrated in [4].

The characteristic equation for the set of equations (1)–(3) was derived and analysed in [2]. Especially illustrative results can be obtained in the case when  $\tau \ll 1$ . The main qualitative conclusions for this regime are virtually independent of  $\tau$ . Keeping this circumstance in mind, in what follows, we present only the results for  $\tau = 0$ .

Let us introduce small deviations  $e$ ,  $n$ , and  $n_f$  from the equilibrium parameters of stationary lasing  $E_{st}$ ,  $N_{st}$ , and  $N_{fst}$  in the form:  $E = E_{st}(1 + e)$ ,  $N = N_{st}(1 + n)$ , and  $N_f = N_{fst}(1 + n_f)$ . We will search for these small deviations assuming that  $e$ ,  $n$ ,  $n_f \sim \exp(\lambda t - iQx)$ . Then, linearizing Eqs. (1)–(3), we arrive at the dispersion equation:

$$a_3 \lambda^3 + a_2 \lambda^2 + a_1 \lambda + a_0 = 0, \quad (4)$$

where

$$a_3 = 1 + \frac{\tau N_{fe} I_{st} v \delta}{(1 + I_{st} \delta)^3};$$

$$a_2 = 1 + I_{st} - \frac{N_{fe} I_{st} v \delta}{(1 + I_{st} \delta)^2} \left[ 1 - \frac{\tau(1 + I_{st})}{1 + I_{st} \delta} \right];$$

$$a_1 = Q + Av I_{st} (1 + I_{st}); \quad a_0 = Q(1 + I_{st});$$

$$A = \frac{N_e}{(1 + I_{st})^2} - \frac{N_{ef} \delta}{(1 + I_{st} \delta)^2}.$$

Equation (4) has two complex-conjugate roots and one real root, which will be denoted below as  $\lambda_{1,2} = R \pm iQ$  and  $\lambda_3 = L$ . Typical dispersion curves are presented in Fig. 1. Fig. 1a shows the evolution of autowaves for  $v = 8$ . One can see that autowaves may arise if their wavelengths are less than some critical length  $\Lambda_{cr}$  of the relevant bifurcation. However, the wavelength of autowaves is not limited from below. The increment  $R$  of autowaves grows as the wave number  $Q$  increases from zero (at the bifurcation point), asymptotically approaching some constant value  $R_\infty$ . Consequently, a whole family of autowaves with arbitrary  $Q > Q_{cr}$  may arise in a laser if some special precautions are not taken.

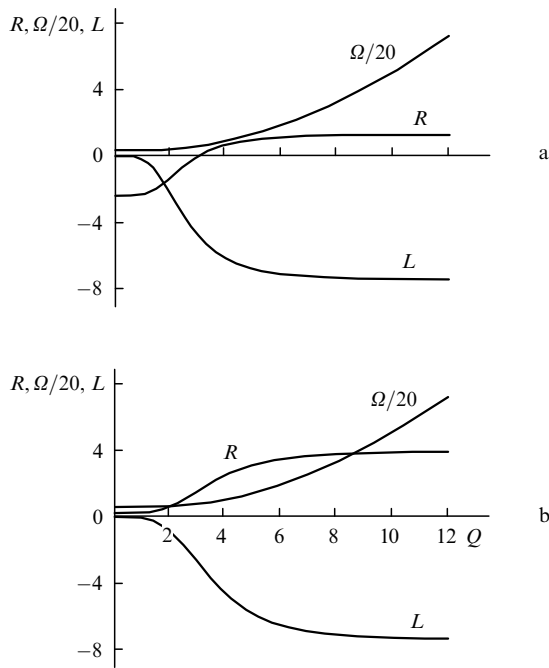


**Figure 1.** The increment  $R$  and the frequency  $\Omega$  of autowaves and the negative root  $L$  of the dispersion equation as functions of the wave number  $Q$  for  $N_e = 10$ ,  $N_{fe} = 7$ ,  $\delta = 3$ , and  $v = 8$  (a) and 30 (b).

For  $v = 30$  (Fig. 1b), the gain of autowaves is positive for any spatial frequency, increasing with the growth in the spatial frequency. Pulsed, rather than autowave, lasing occurs in this regime. The increment of perturbations is positive for any wavelength of these perturbations, including infinitely large wavelengths. Detailed calculations demonstrate that the optical field virtually simultaneously increases and decays within the entire laser aperture [3].

Fig. 2 displays the increment of autowaves  $R$  as a function of parameters  $v$  and  $Q$ . This plot shows that, as  $v$  increases, the

region of positive  $R$  expands, reaching the coordinate  $Q = 0$ . Pulsed lasing builds up in the system when this point is reached.

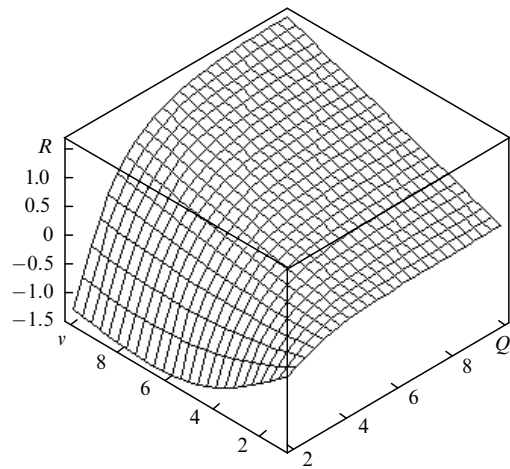


**Figure 2.** The increment  $R$  of autowaves as a function of the parameters  $v$  and  $Q$  for the conditions of Fig. 1.

### 3. Competition of autowaves in a laser under different conditions

The spectral dependences calculated above allow us to find the increment of autowaves for an idealised case of an infinite aperture. For any real conditions, the choice of the frequency of autowaves depends on many factors. Specifically, detailed calculations of the optical field in a one-dimensional open cavity have revealed the presence of a system of autowaves with approximately equal frequencies and wavelengths in a laser [3]. This finding indicates the existence of selective factors, which may be associated with losses through open sides of the cavity and diffraction from aperture edges.

More definite conclusions concerning the behaviour of spectral components can be made if we ensure resonant conditions for autowaves. In particular, a cavity with reflecting side walls can be employed. A discrete set of harmonics will be excited in a laser then, with an integer number of half-waves falling within the aperture. Calculations for a broad range of parameters were performed in order to investigate this situation.

An iteration procedure similar to the method described in [3], but modified to include the presence of side walls was used in these calculations. The equation for a single cavity round trip was solved at each iteration using an implicit difference method (a nonmonotonic sweep method involving the Crank–Nicolson scheme). The active and nonlinear media were considered as infinitely thin amplitude–phase screens placed adjacent to a semitransparent mirror. The intensities thus determined were then used to solve kinetic equations (2) and (3). The boundary condition on the side walls was written as  $\partial E / \partial x|_{x=\pm a} = 0$ , which corresponds to a total specular reflection.

Typical results of these calculations are presented in Fig. 3. For the situation illustrated in Fig. 3a, the initial field was represented as a sum of harmonics:

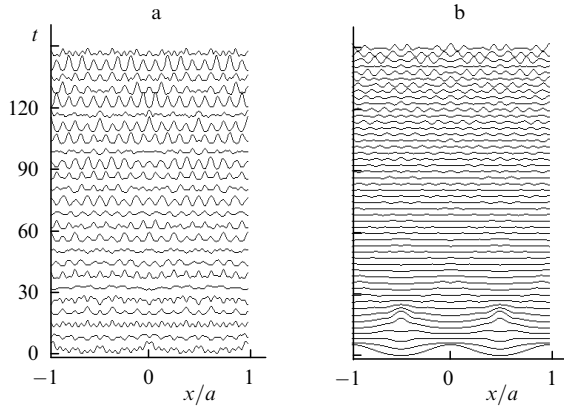


**Figure 3.** The profile of an optical field at different moments of time in a cavity with mirror side walls for the conditions of Fig. 1a with the initial field defined by Eq. (5) (a) and Eq. (6) (b). The time variable in Figs. 3–5 is normalised to the total round-trip time.

$$E(x) = E_{st} \left( 1 + 0.2 \sum_{m=1}^5 \cos \frac{2^m \pi x}{2a} \right). \quad (5)$$

One can see from Fig. 1a that harmonics with  $Q < Q_{cr} \approx 3$  should decay as functions of time. This condition is satisfied for the first three harmonics in Eq. (5), since  $Q = 0.65, 1.3,$  and  $2.6$  for  $m = 1, 2,$  and  $3$ . Fig. 3a shows that these harmonics decay with time, while two harmonics with the highest orders (among the harmonics constituting the initial field) experience amplification and completely determine the field profile. One can also notice that oscillations with shorter wavelengths also arise and build up.

In the regime illustrated in Fig. 3b, the initial field is written as

$$E(x) = E_{st} \left( 1 + 0.6 \cos \frac{2\pi x}{a} \right). \quad (6)$$

In this case, the wavelength corresponds, in accordance with Fig. 1a, to a decaying harmonic. This decay occurs after  $\sim 20$  cavity round trips. Under these conditions, high-frequency oscillations arise in the profile of a uniform field. Amplification of these oscillations results in a strong modulation of the optical field after  $\sim 100$  cavity round trips.

Hence, it is unlikely that the considered closed cavity may ever allow efficient spectral selection of autowaves. However, several simple measures can be taken in this case. In particular, by choosing the material of the walls with appropriate properties, the magnitude of losses for high-order autowave modes can be increased. One can also choose a suitable profile of the walls for this purpose (e.g., a section with a discontinuity of side walls would introduce considerable losses for high-order harmonics).

Along with a system with ‘mirror’ boundary conditions, a laser with periodic boundary conditions

$$E, N, N_f|_{\phi=0} = E, N, N_f|_{\phi=2\pi},$$

$$\left. \frac{\partial E}{\partial \phi}, \frac{\partial N}{\partial \phi}, \frac{\partial N_f}{\partial \phi} \right|_{\phi=0} = \left. \frac{\partial E}{\partial \phi}, \frac{\partial N}{\partial \phi}, \frac{\partial N_f}{\partial \phi} \right|_{\phi=2\pi}.$$

has been also considered. Such a model of a laser can be easily implemented by using a two-dimensional ring-shaped

semitransparent mirror with an inner radius  $r_1$  and an outer radius  $r_2$  and a reflection coefficient  $R_1(r)$  and employing an active medium whose cross section has a shape of a similar ring. The reflection profile of the mirror was smoothed up around the edges. The radial dependence of the reflection coefficient can be written in this case as  $R_1(r) = R_0$  for  $r_1 < r < r_2$  and  $R_1(r) = R_0 \exp[-(r - r_{1,2})^2/d^2]$  around the inner and outer edges, respectively. Our simulations have shown that the specific form of the function chosen to smooth the reflection profile up is not very important. It was assumed also that the Fresnel parameter is  $N_F = 40$ ,  $r_1 = 0.66a$ ,  $r_2 = 0.94a$ , and  $d = 0.04a$ . The second mirror was assumed to be totally reflecting and infinite.

We deal with a two-dimensional problem in the case under study. However, the width of the ring mirror was chosen not very large, and the field had a simple structure along the radius (similar to a single-mode regime). As a result, the field distribution along one of the axial coordinates can be easily calculated. The resonant properties of autowaves in this regime were similar to the resonant properties of autowaves in the one-dimensional case. There are two differences of the problem under study from the corresponding one-dimensional problem. The first difference is that the system is characterised by losses due to the leaking of the optical field in the radial direction. Therefore, we cannot perform an exact comparison of the results of two-dimensional analysis with the results of one-dimensional consideration. However, taking these additional losses into account, we can reduce losses due to the coupling of radiation out of the system through the semitransparent window and examine qualitatively the same lasing regimes as above.

The second difference of the considered problem from the one-dimensional case is that the trajectories of autowaves deviate from straight lines, which gives rise to the leaking of autowaves through the outer edge of the ring mirror. The autowave-modulated optical field is also shifted along the propagation direction of autowaves, which results in a partial leaking of this field in the same direction.

Figs. 4 and 5 display typical results of calculations for the laser field under the above-specified conditions. Autowaves running only in one direction were simulated in these calculations for the sake of clarity by assuming that the phase of the initial field is equal to the polar coordinate  $\alpha$ . Figs. 4a and 5a show the cross sections of the field at different moments of time by a circumference with a radius equal to  $0.8a$ , i.e., the field distribution along the central line of the

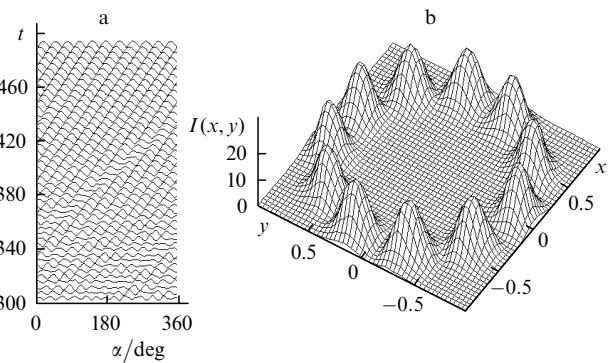


**Figure 4.** The profile of an optical field at different moments of time along a circumference with a radius equal to  $0.8a$  (a) and field distribution (b) simulated for  $v = 4$ ,  $N_e = 20$ ,  $N_{fc} = 14$ ,  $\delta = 3$ , and  $\varepsilon = 0.3$ .

ring mirror. Figs. 4b and 5b present the simulated transverse intensity profile of a laser beam. One can see that a ring-shaped periodic light structure rotating with a constant speed arises in a laser. The initial light field was taken in the form of a step:  $E(r, \phi) = (1 \pm \varepsilon)E_{st}$  for  $x < 0$  and  $x > 0$ , respectively. Therefore, ordered structures were produced exclusively due to the intrinsic properties of the system under consideration.

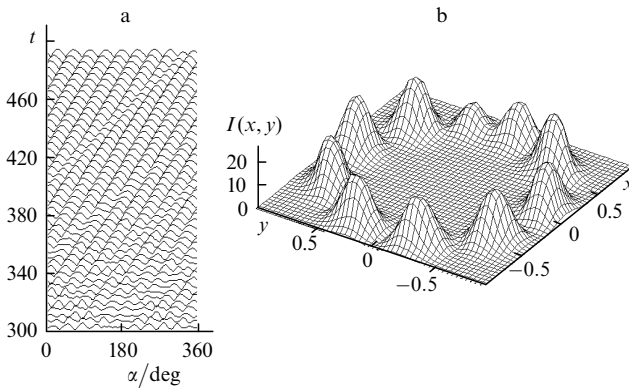


**Figure 5.** The profile of an optical field at different moments of time along a circumference with a radius equal to  $0.8a$  (a) and field distribution (b) simulated for  $\nu = 6$ ,  $N_e = 20$ ,  $N_{fc} = 14$ ,  $\delta = 3$ , and  $\varepsilon = 0.1$ .

Figs. 4a and 5a show how a quasi-periodic field emerges from a steplike field distribution and how this quasi-periodic field evolves in time, acquiring a profile close to the profile of a single harmonic. Under conditions of Fig. 4, a field profile similar to the profile of an ideal harmonic is achieved. Under the conditions of Fig. 5, the periodicity is perturbed: one of the wave periods is partially doubled. A more detailed analysis of this regime has shown that the dependence of the intensity on the angular coordinate becomes virtually exactly periodic after  $\sim 200$  iterations.

The results of these simulations demonstrate that a coaxial laser is characterised by a strong spectral selection of autowaves. Both high- and low-frequency spectral components are suppressed in such a system, and only one harmonic survives. One can see from Figs. 1–3 that only low-frequency perturbations are suppressed in lasers with an infinite aperture or ideal side mirror walls. Comparison of these results suggests that high-frequency autowaves are suppressed due to the choice of the cavity shape. Obviously, high-frequency components of autowaves produce rays with a considerable transverse component of the wave vector, i.e., rays with a considerable tilt, in the optical field. Such rays rapidly escape from the ring-mirror cavity in the lateral direction, i.e., in the direction of leaking of high-frequency autowaves.

The rotating optical field obtained in our simulations is similar to some extent to a spiral light field [5]. Visually, this field is reminiscent of the so-called multipass modes (M modes) of a stable cavity [6]. However, autowave light structures differ from spiral beams by their properties and their origin. First, an autowave profile is always strongly modulated, while spiral beams are not necessarily modulated. Second, an autowave profile is a nonstationary running or standing structure, while spiral beams are usually stationary. In this paper, we investigated the light field in a Fabry–Perot cavity rather than in a stable cavity. Therefore, the main spatiotemporal features of the optical field are due to the interaction of rays with an autowave profile rather than

due to the cavity geometry. When both of these two factors (the presence of autowaves and the stable cavity geometry) are important, the scenario of lasing becomes much more complicated. This situation requires further analysis.

## 4. Conclusions

The results obtained in this paper allow us to conclude that an autowave profile of the optical field with a broad spatial spectrum may arise in a wide-aperture laser with a saturable absorber above the bistability threshold. Boundary conditions on the side walls of the cavity play a dominant role in the formation of the spectrum of these autowaves.

Apparently, quasi-stationary quasi-periodic autowaves arise in an open cavity due to the competition of the amplification of autowaves and the losses of autowaves through the side boundaries of the active volume. As one might expect, the set of autowaves arising in cavities with mirror side walls is characterised by discrete frequencies and the presence of a lower bound in spatial frequency. Spectrum control in this case requires special measures. In particular, the properties and the geometry of side walls can be chosen in a proper way.

A high efficiency of spectral selection of autowaves is achieved when these waves propagate along a closed trajectory, as in the case of a coaxial laser. Calculations performed in this paper demonstrate that, starting with an arbitrary initial field, such a system may produce a single autowave mode reminiscent in its form of an ideal harmonic. It seems of considerable interest to investigate such a laser field within a broad range of geometric parameters of the cavity, especially in the case of a stable cavity. Apparently, such optical fields can be also generated due to autowaves of some other nature, e.g., in the case when a phase nonlinear medium is placed inside a cavity.

## References

1. Rozanov N N *Opticheskaya Bistabil'nost' i Gisterezis v Rasprede-lennykh Nelineynykh Sistemakh (Optical Bistability and Hysteresis in Distributed Nonlinear Systems)* (Moscow: Nauka, 1997)
2. Zaikin A P, Molevich N E *Kvantovaya Elektron.* **24** 908 (1997) [*Quantum Electron.* **27** 882 (1997)]
3. Zaikin A P, Molevich N E *Kvantovaya Elektron.* **29** 114 (1999) [*Quantum Electron.* **29** 952 (1999)]
4. Zaikin A P *Kvantovaya Elektron.* **25** 867 (1998) [*Quantum Elec-tron.* **28** 843 (1998)]
5. Abramochkin E, Losevsky N, Volostnikov V *Opt. Commun.* **141**, 59 (1997)
6. Korolenko P V, Fedotov N N, Sharkov V F *Kvantovaya Elektron.* **22** 562 (1995) [*Quantum Electron.* **25** 536 (1995)]